Polymer 51 (2010) 4994–5001

Contents lists available at ScienceDirect

Polymer

journal homepage: www.elsevier.com/locate/polymer

Surface-induced phase transitions in dense nanoparticle arrays of lamella-forming diblock copolymers

Shiben Li [a,*], Yongyun Ji [a], Peng Chen [b], Linxi Zhang [a], Haojun Liang [c]

[a] Department of Physics, Wenzhou University, Wenzhou, Zhejiang 325035, China
[b] School of Chemistry, Anhui University, Hefei, Anhui 230039, China
[c] CAS Key Laboratory of Soft Matter Chemistry, University of Science and Technology of China, Hefei, Anhui 230026, China

ARTICLE INFO

Article history:
Received 21 January 2010
Received in revised form
19 July 2010
Accepted 9 August 2010
Available online 14 August 2010

Keywords:
Phase transition
Diblock copolymer
Nanoparticle array

ABSTRACT

The surface-induced phase transitions in dense nanoparticle arrays of lamella-forming diblock copolymers are investigated by using the real-space self-consistent field theory. The dense nanoparticle array provides a distinct and strong confinement environment where there are incomplete confinements in three spatial directions. Several complicated phases with cubic symmetries, such as the monocontinuous and bicontinuous phases, are identified in the dense nanoparticle arrays. Through adjusting the strength of surface preference, the disorder phases are induced into the complicated order phases in the nanoparticle arrays with small periods while the order–order transitions occurs in those with large periods. Investigations on the free and entropic energies indicate that these surface-induced phase transitions are of first-order and the stabilities of order phases are intimately correlated to the strength of surface preference. Our results enrich the knowledge about the phase behaviors of macromolecules in confined systems, which may be helpful to fabricate the novel nanomaterials based on the block copolymers.

1. Introduction

The linear AB diblock copolymers spontaneously form various phases in bulk, such as the lamellar, cylindrical, spherical and more complex phases, depending on two phase parameters, the block ratios and interaction energies. The phase transitions, including the order–order transition (OOT) and order–disorder transition (ODT), occur in the bulk diblock copolymer system, responding to the alteration of these two phase parameters, especially of the interaction energies between the blocks that controlled by the temperature [1–3]. Investigation on such phase transitions is not only a basic problem involved in interdisciplinary knowledge, but is also driven by a wealth of potential technological applications [4–6]. However, introducing the confinement surfaces, such as thin films, cylindrical pores and spherical cavities, can strongly influence the phase behaviors of diblock copolymers by varying the confinement sizes and the short-range fields on the confinement surfaces [7]. Therefore, the confinement surface can be regarded as another phase parameter to control the phase transitions of confined diblock copolymers in addition to their bulk phase parameters, which have been demonstrated to be an efficient approach to obtain the novel phase structures of diblock copolymers.

Usually, the thin films, cylindrical pores or the spherical cavities provide the confinements with their inner surfaces where the polymers are packed into a certain space. The thin film offers an ideal template to test the confinement effects for the diblock copolymers, which have attracted enormous contributions in the theoretical, experimental and simulation's sides [8–23]. Under this one-dimensional confinement, the bulk parallel lamellae can be compressed or stretching, or even can be induced into the perpendicular lamellae or the mix lamellae when the confinement sizes are changed or the strengths of surface fields are increased to the suitable values [10–12,15,16,18]. Specifically, Tang has constructed the phase diagrams of diblock copolymers in thin films arranged as strengths of top and bottom surface tensions where the parallel, perpendicular and mix lamellae have been discussed in detail [12]. For the confinement-induced effect, it has been convincingly confirmed that as the system switches between two parallel lamellae with unequal lamellar layer number, the first-order phase transition occurs [10]. When the cylinder-forming diblock copolymers are confined in the thin films, a rich variety of morphologies, such as the perforated lamellae and the perpendicular lamellae, can be observed through varying the film thicknesses and strengths of surface preferences [13,14,17,20–22,24]. This variety of morphologies was well demonstrated in the film confinements when the diblock copolymers are located in the phase boundaries in bulk phase diagram [24]. For both the lamella- or

* Corresponding author.
E-mail address: shibenli@wzu.edu.cn (S. Li).

0032-3861/$ – see front matter © 2010 Elsevier Ltd. All rights reserved.
doi:10.1016/j.polymer.2010.08.019

cylinder-forming diblock copolymers, it was believed that the incommensurability between the film thickness and the polymer periods, as well as the preferential surfaces, play an important role in inducing the phase transitions of diblock copolymers in the thin films.

The diblock copolymers undergo another type of incommensurability under the cylindrical pore confinements (that is, the two-dimensional confinement), in which the bulk lamellae are distorted into multiple concentrically cylindrical shells but the cylinder domain submits to a rich variety of distorted morphologies [24–36]. For the concentrically cylindrical shells, their transitions are predicted to be the first-order in Monte Carlo simulation but are argued to be second-order in the strong segregation region by the strong-stretching theory [32]. For the cylinder-forming diblock copolymers, the phase transitions were observed to be controlled with the ratio between the bulk polymer period and the pore diameter. An example is that the structural sequence: a string of spheres, a single cylinder, a straight band, and so on, is observed to be the first-order phase transition as the pore diameter is increased [35]. The phase structures gained in the spherical cavity (three-dimensional confinement) obviously differ from those in thin film and cylindrical pore confinements. For the lamella-forming diblock copolymers, the parallel lamellae in bulk convert into a couple of spherically concentric shells in order to meet the requirement of spherical symmetries, which have been observed in experiments [37–40] and reproduced in simulations under the spherical cavity confinement [41–44]. Specifically, Yu et al. preformed a systematic Monte Carlo (MC) study on the symmetric diblock copolymers confined in spherical nanopores, and they revealed the dependence of morphologies on the surface fields and confinement sizes (that is, the sphere diameter) [43]. The cylinder-forming diblock copolymers exhibit the diversity in the structures when the confinement size was varied, due to the incommensurability between the sphere diameters and the polymer periods [42,44,45]. Our recent research showed the confinement-induced effects on the phase structures of cylinder-forming diblock copolymers under spherical confinements where the bulk cylinders can be packed into the multilayered structures [46]. We note that under spherical confinement the commensurability requires the number of multilayered structures n for either the cylinder-forming or the lamella-forming diblock copolymers obeys the expression, $d/L_0 \approx 2(n-1)$, where d is sphere diameter and L_0 represents the bulk polymer periods [43,46]. This expression has the similar format for those obtained in the thin film confinement where the diameter is increased to infinite, indicating that the diblock copolymers have the similar behaviors in the limiting case [8].

Recently, we introduce the nanorod-array confinement where the confinements are provided by the outer surfaces of nanorods and consequently the confinements are incomplete in two spatial directions [47,48]. Under this special confinement, the increasing of nanorod diameter not only leads to a crowded confinement space, but also results in the variation of confinement dimensions. The results indicate that the surface field, that is, the preferential surface, induces the phase transitions among a series of distorted lamellar structures in the nanorod array with a certain diameter of nanorod [47]. Furthermore, investigation on the free energies also indicates that there is first-order phase transition for the lamella-forming diblock copolymers in nanorod arrays [48]. Other than the nanorod-array confinement, the nanoparticle array provides another type of the outer surface confinement wherein the confinement dimensions are also fractional but the particle surfaces are spherical symmetries. We are aware that the dense nanoparticle array can be constructed by the colloidal crystal template in experiment, and the unexpected phases can be detected by the transmission electronic micrograph [38]. It is interesting to explore how the diblock copolymer behaves in such nanoparticle arrays. In the present work, we employ the self-consistent field theory (SCFT) calculation method to investigate the phase transitions for the lamella-forming diblock copolymers confined in the dense nanoparticle arrays, in which the nanoparticles are compactly arranged with a periodic cube method. By varying the strength of surface preference, we mainly concentrate on the ODT and OOT processes of diblock copolymers in the dense nanoparticle arrays with several values of array periods. It is expected to observe the novel phase structures and the corresponding phase behaviors for the lamella-forming diblock copolymers in this unique confinement system when the strengths of surface preferences are increased.

In the next section, we will present the model and outline the SCFT calculation method. In the third section, we mainly focus on the novel phase structures and discuss the surface-induced ODTs in the nanoparticle arrays with small periods and the surface-induced OOTs in the arrays with relatively large periods, respectively. Conclusions are presented in the last section.

2. Model and method

We consider a system of AB diblock copolymers confined in a nanoparticle array where the nanoparticles are cubically arranged and the neighboring nanoparticles contact each other, as shown in Fig. 1a. This type of nanoparticle array provides a unique confinement, in which the diblock copolymers are incompletely confined at three spatial directions, similar to the nanorod-array confinement [47,48]. To illustrate this incomplete confinement in detail, we plotted the cross-section at $z = 0.50D$, as shown in Fig. 1b. This cross-section shows that each nanoparticle contacts with its neighboring ones at eight contact points, which are released at the

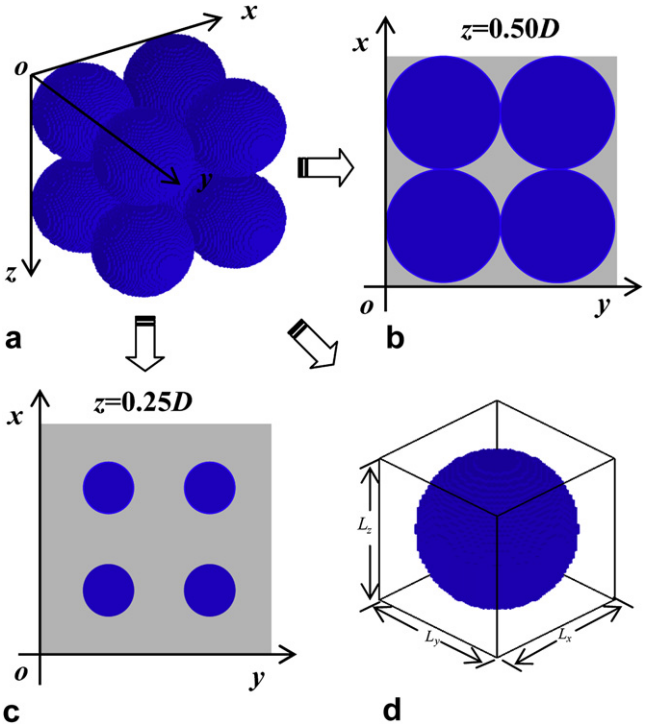

Fig. 1. Calculation model. (a) The sketch map of dense nanoparticle array. The spherical nanoparticles are packed into a cubic arrangement. (b) A cross-section view at $z = 0.5D$. (c) A cross-section view at $z = 0.25D$. (d) The cubic unit used in the SCFT calculations. Here, the unit lengths at three directions are L_x, $L_y$and L_z($L_x = L_y = L_z = D$), respectively.

other positions. For example, when the cross-section moves up to another position, $z = 0.25D$, as shown in Fig. 1c, the confinement space becomes larger and the connective point disengages. This phenomenon is attributed to the spherical symmetry of nanoparticle, obviously differs from the array confinement provided by the nanorods having cylindrical symmetries [47]. We performed the SCFT calculation in a cube with the size of $L_x = L_y = L_z = L$, as shown in Fig. 1d, in which the nanoparticle diameter is to be $D = L$. In the calculation processes, the periodic boundary conditions (PBCs) are selected to construct the whole nanoparticle array. Since the mismatch between the PBC and the period of bulk lamella will result in an artifact structure corresponding to a system of infinite size, and consequently the match between the periods of bulk lamella and the PBCs is crucial to obtain meaningful results [11,49]. Here, we choose the calculation unit with the size of $L = nL_0$ where n is integer, in order to meet such a match.

Based on the Gaussian chain model, the SCFT is a successful theoretical method for studying phase behaviors of block copolymers. The diblock copolymers in the nanoparticle array are regarded as Gaussian chains with the volume fraction of A-blocks, f_A, and polymerization index, N. The repulsion interactions between the A and B blocks are parameterized with χN where χ is the Flory–Huggins parameter. The basic treatment in SCFT is that the multi-body repulsion interactions between the A and B blocks are replaced by a mean field $\omega_{A(B)}$. In a confined space with volume V and preferential surface, the SCFT free energy per chain of diblock copolymers (in the unit of k_BT) can be expressed as [24,50]

$$\frac{F}{nk_BT} = -\ln\left(\frac{Q}{V}\right) + \frac{1}{V}\int dr[\chi N\phi_A\phi_B - \omega_A\phi_A - \omega_B\phi_B - U_A\phi_A - U_B\phi_B - P(\phi_0 - \phi_A - \phi_B)], \quad (1)$$

where $\varphi_{A(B)}$ is the segment density field, and the single chain partition function, Q, can be expressed as $Q = \int q(\mathbf{r},1)d\mathbf{r}$ in the mean fields $\omega_{A(B)}$. The segment distribution function, $q(\mathbf{r},s)$, is the statistical weight of a chain segment of contour length s containing a free chain end with its connected end located at $\mathbf{r}$, which satisfies the modified diffusion equation in the mean fields, that is, $\frac{\partial}{\partial s}q(\mathbf{r},s) = R_g^2\nabla^2 q(\mathbf{r},s) - N\omega q(\mathbf{r},s)$ with the initial condition $q(\mathbf{r},0) = 1$. Since the diblock copolymer is asymmetric, another segment distribution $q'(\mathbf{r},s)$ is necessary, which satisfies the modified diffusion equation multiply -1 in left hand, and with the initial condition, $q'(\mathbf{r},1) = 1$. In the modified diffusion equations above, R_g is the gyration radius of an ideal Gaussian chain for the diblock copolymer, and $\omega = \omega_A$ for $0 \le s \le f_A$; otherwise, $\omega = \omega_B$. The Crank–Nicholson scheme is used to solve the modified diffusion equation. $U_{(A,B)}$ represents the surface preference, which is a short-range surface field with non-negative value engendering on the lattice next to the boundaries outside the nanoparticles. Moreover, a Lagrange multiplier, P, is introduced into the calculations in order to ensure the incompressibility of the system. We generalize the incompressibility constraint to $\varphi_0 = \varphi_A + \varphi_B$ and $\varphi_0 = 1$ outside the nanoparticles, $\varphi_0 = 0.5$ in the lattice next to the boundaries, and $\varphi_0 = 0$ inside the nanoparticles. These generalizations ensure the representation of an impenetrate boundary and cause the diblock copolymers confined in the nanoparticle array.

In order to obtain the equilibrium phase, the free energy is minimized to a stable value with respect to the mean fields and the segment density fields. The minimization of free energy results in a set of self-consistent equations, which can expressed as

$$\omega_A(\mathbf{r}) = \chi(\phi_B(\mathbf{r}) - f_B) - U_A(\mathbf{r}) + P(\mathbf{r}), \quad (2)$$

$$\omega_B(\mathbf{r}) = \chi(\phi_A(\mathbf{r}) - f_A) - U_B(\mathbf{r}) + P(\mathbf{r}), \quad (3)$$

$$\phi_A(\mathbf{r}) = \frac{V}{Q}\int_0^{f_A} dsq\,(\mathbf{r},s)\,q'\,(\mathbf{r},s), \quad (4)$$

$$\phi_B(\mathbf{r}) = \frac{V}{Q}\int_{f_A}^{1} dsq\,(\mathbf{r},s)\,q'\,(\mathbf{r},s). \quad (5)$$

These equations can be numerically solved by a combinatorial screening method based on the real-space implementation originally proposed by Fredrickson and Drolet [50,51]. The real-space implementation is suitable for exploring the novel phase structures of copolymers without requiring assumptions of system symmetry. In this research, we employ the real-space implementation to search for the phases with minimum free energies; each minimization is run several times using different random initial mean fields ω_A and ω_B to ensure that the exact equilibrium structure is obtained.

To investigate the different effects of surfaces preferential to the minority and majority blocks, we choose a slight asymmetric diblock copolymer with volume fraction of $f_A = 0.4$ and incompatible degree of $\chi N = 40$. The diblock copolymers with these parameters exhibit a rigid lamellar characteristic in the bulk, having the lamellar period of $L_0 = 4.40R_g$, which is similar to the nanorod-array confinement cases [47]. This similar choice of polymer parameters provides an opportunity to compare their main features of diblock copolymer phase structures between these two systems. The main purpose of this work is to obtain the surface-induced phase behaviors of lamella-forming diblock copolymers so that we reduce the strength of surface preference to be $\lambda_{A(B)} = U_{A(B)}/\chi N$ for either A- or B-preferential surface and increases $\lambda_{A(B)}$ at a small step of $\Delta\lambda_{A(B)} = 0.05$. In the present work, we increase the cubic unit size L from L_0 only up to $3L_0$ because the large unit size requires a dramatic increasing for the computer capability. In all calculations, we assigned $0.2R_g$ as the lattice constant; we divided the chain contour length into 200 segments and performed the SCFT calculations in a PC cluster with 25 nodes.

3. Results and discussion

We investigate the surface-induced phase transitions of diblock copolymers confined in the particle arrays with periods of L_0, $2L_0$ and $3L_0$, in which have the volumes in per calculation unit of about $0.48L_0^3$, $3.81L_0^3$ and $12.87L_0^3$, respectively (see Fig. 1d). It is reasonable to designate the arrays with periods of L_0 and $2L_0$ as the arrays with small period and the array with period of $3L_0$ as the array with large period. The surface fields play important role in inducing the phase transitions of diblock copolymers in the thin film, cylindrical pore and nanorod-array confinements [12,29,47,48]. We are expected to obtain the different structures of diblock copolymers in the arrays with the small and large periods. The phase structures observed in the arrays with small and large periods are sorted into several groups. These structures are presented in the form of three different colors (red, green and blue), representing the density distributions of the monomers belonging to A block, B block, and nanoparticles, respectively. In the subsections, we will first discuss the phase structures and then investigate the phase transitions of lamella-forming diblock copolymers in the nanoparticle arrays with the small periods in subsection 3.1 and the arrays with the large periods in subsection 3.2.

3.1. The ODTs in the arrays with small periods

In the arrays with small periods, there is comparatively crowded space for assembly of diblock copolymers. For the A-preferential surfaces, we observe two types of phase structures in the arrays with small periods, as shown in Fig. 2a. One phase is the disorder (DIS) phase where the segments are distributed randomly in the nanoparticle arrays. It is well known that the DIS phase of diblock copolymers occupies a relatively most phase space in bulk phase diagram arranged as the volume fraction and incompatibility degree, which has been investigated by the SCFT and MC methods [52,53]. In bulk, the DIS phase originates from the obvious asymmetry about two blocks or high temperature of system. Under the cylindrical pore or spherical cavity confinements, the DIS phases have not been reported as far as we know, probably due to the comparatively large sizes of confinements the previous studies adopted [24,30,43,46]. For example, Yu et al. reported the most crowed spherical space with diameter of $d = 1.5L_0$ where the volume of confinement is about $1.77L_0^3$ [43]. Under this crowed confinement, they observed the parallel lamellae instead of DIS phases. Here, we reported the DIS phases in the nanoparticle-array confinements provided by the outer surfaces where the ordered distribution of segments in bulk lamella disappears into the disordered ones because of the severe confinement conditions, that is, the volume of the space constructed by the eight dense arrays is about $0.48L_0^3$. Actually, we have also observed a similar DIS phase of diblock copolymers confined in the nanorod arrays when the diameter of nanorod excesses the 41 percent of nanorod array period [47]. The other phase is an order phase, designated as SA_B-LN_A, in which the B-block domains are packed into a periodic sphere array (SA_B structure) in the whole nanoparticle array. On the other hand, the A-block matrix is adsorbed into the nanoparticle surfaces and connects with the neighboring units at three spatial directions, constructing a lamella network (LN_A structure) in the whole nanoparticle array. Actually, the SA_B-LN_A phase is a mono-continuous structure possessing a cubic symmetry in the whole array. Certainly, the cubically arranged nanoparticles result in the cubic symmetry about the diblock copolymers confined in the array. It is worthwhile to note that the SA_B-LN_A structure differs from the well-known sphere phase in bulk system where the minority block domains are packed into a body-centered cubic arrangement. Here, we observe the SA_B-LN_A structure with the cubic arranged spheres constructing from the B-blocks, which provides an opportunity to fabricate the nanoparticle arrays through the self-assembly of block copolymers.

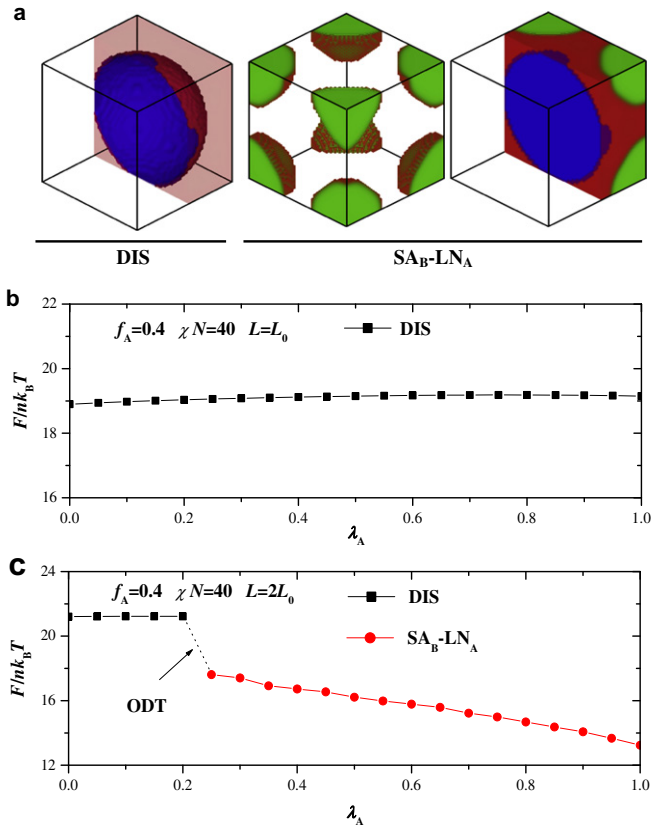

Fig. 2. The phase structures in the arrays with periods of $L = L_0$ and $L = 2L_0$ and phase transitions induced by A-preferential surfaces. (a) The phase structures observed in the arrays with periods of $L = L_0$ and $L = 2L_0$.(b) The free energy, F/nk_BT, as function of the strength of surface preference, λ_A, in the arrays with periods of $L = L_0$ and A-preferential surfaces. (c) The free energy, F/nk_BT, as function of strength of surface preference, λ_A, in the arrays with periods of $L = 2L_0$ and A-preferential surfaces.

Fig. 2b and c show the free energies, F/nk_BT, as function of strength of surface preferences, λ_A, for the diblock copolymers confined in the arrays with small periods and A-preferential surfaces. Fig. 2b indicates that the DIS phase appears in the array with period of L_0 and A-preferential surfaces, which is independent of the strengths of surface preferences. In other words, the DIS phase is insensitive to the strength of surface preference in such crowded confinement space. Furthermore, the nearly unchanged free energy curve indicates that there is not phase transition in this case. In addition, we have checked the B-preferential surfaces, and the similar results were obtained. The insensitivity of DIS phases on preferential surface is probably due to the crowded space caused by the small period. Specifically, in this crowed space, the total energies of surface-polymer interactions are relatively small because of the relatively small surface of nanoparticles, leading to the insensitivity of DIS phases on the preferential surface. When the array period is increased to be $2L_0$, the diblock copolymers exhibit the different phase transition behaviors in the nanoparticle arrays with A-preferential surfaces, as shown in Fig. 2c. Once again, we observed the DIS phase at the weak strength of surface preference. However, the DIS phase can transit into an order phase, the SA_B-LN_A phase, when the surface preference is increased to the certain strength. This phase transition is clearly displayed in Fig. 2c, wherein an abrupt change of free energy occurs at the point of $\lambda_A = 0.2$. The abrupt jump of free energy indicates a signal of first-order phase transition for the diblock copolymers confined in the nanoparticle arrays with small periods. Moreover, it is convincing that the obvious structural variations appear in this first-order ODT process. Originally, the segments of diblock copolymers distributes randomly in the crowded confinement space, exhibiting the DIS phase, and subsequently the preferential surface enforces the A-blocks into the surfaces orderly when $\lambda_A$increases. As a result, the long-range order structure, that is, the SA_B-LN_A phase, is induced through the preferential surfaces when the strength of surface preference is strong enough.

The slight asymmetry of two blocks enables us to investigate the phase structures and the corresponding phase behaviors of diblock copolymers confined in the nanoparticle arrays with different preferential surfaces. For the arrays with B-preferential surfaces, we observe another order phase structures in the array with period of $2L_0$, as shown in Fig. 3a. In the A-block domain, the bulk lamella structures are pushed into the unit edges, which forms several cylinder-like structures and construct the cylinder network (CN_A structure) in the whole array. On the other hand, the B-block domain distributes near the nanoparticle surfaces, which forms the concentric lamellae (CL_B structure) with a somewhat connectivity with each other, as shown in Fig. 3a, due to the B-preferential

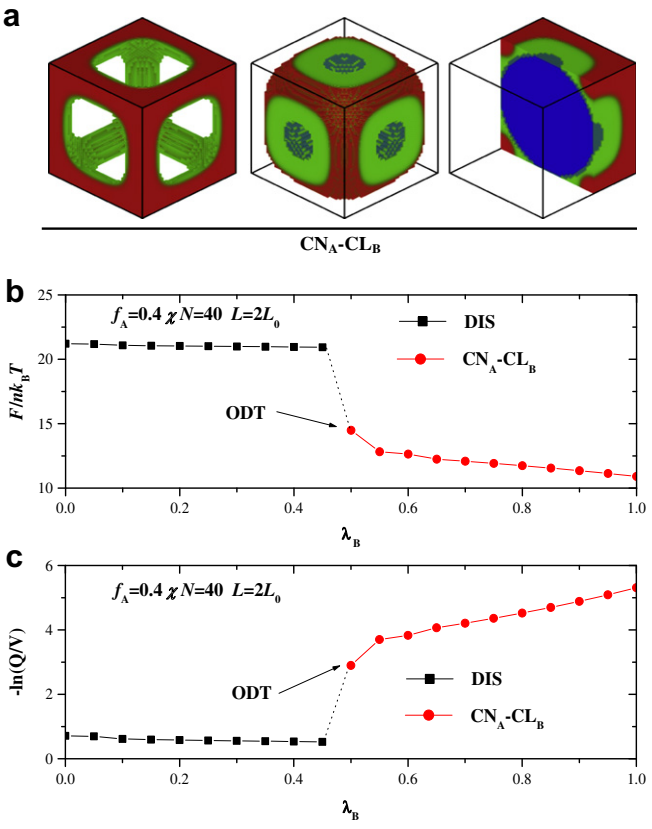

Fig. 3. The phase structures in the arrays with periods of $L = 2L_0$ and phase transitions induced by B-preferential surfaces. (a) The phase structures observed in the arrays with periods of $L = 2L_0$.(b) The free energy, F/nk_BT, as function of strength of surface preference, λ_B, in the arrays with periods of $L = 2L_0$ and B-preferential surfaces. (c) The entropic energy, $-\ln(Q/V)$, as function of strength of surface preference, λ_B, in the arrays with periods of $L = 2L_0$ and B-preferential surfaces.

surfaces. We note that the CN_A-CL_B phase is a bicontinuous network structure where both the A and B block domains are periodically continuous at three spatial directions. Actually, several bicontinuous network structures, such as the plumber's nightmare structure, have been reported in the previous works for the diblock copolymers in the bulk system [54–56], which can be explained by the mathematical description through the minimal surfaces and spatial symmetry [57,58]. Here, the CN_A-CL_B phase is caused by the preferential surface that provides the adsorption energy instead of the entropic force.

For the B-preferential surfaces, we investigate the phase transitions in the arrays with period of $2L_0$, the small period array, as shown in Fig. 3b and c. Fig. 3b shows F/nk_BT as function of λ_B. The results indicate that the weak B-preferential surface does not influence the DIS phase. When λ_B is increased to a certain value, the phase transition occurs at $\lambda_B = 0.45$, as shown in Fig. 3b. Similarly, this phase transition is also of first order, since the second-derivate of free energy is discontinuous. We are aware that the value of phase transition point is bigger than those obtained in the A-preferential surfaces. This fact reminds us that it needs stronger strength of surface preference to engender the phase transition in this case. This is due to the entropic effect caused by the asymmetric diblock. The minority block prefers to the neutral surface, which is called "hard-wall" effect [59], so that it needs stronger λ_B to overcome the spontaneous distribution of minority blocks on the surfaces. In another word, the hard-wall effect produce an additional entropic force only for adsorbing the minority blocks (A-blocks), therefore it need relatively weak λ_A to realize the ODT process. Furthermore, we plotted the entropic energy, $-\ln(Q/V)$, as function of λ_B in Fig. 3c. The result further indicates the first-order phase transition occurs at this ODT process. On the other hand, it is naturally that the CL_B structure and consequently the CN_A-CL_B phase, will be more stable with the increasing λ_B, because the surface adsorbs the corresponding blocks more tightly. The evidence is shown in Fig. 3c where the entropic energy increases with λ_B.

We would like to summary several characteristics of phase transitions in the nanoparticle arrays with small periods. The most outstanding feature is that the preferential surface induces the ODTs in the nanoparticle arrays with small periods. The previous works have reported that the ODT is the first order for the asymmetric diblock copolymers but is the second order for the symmetric diblock copolymer in the thin film and spherical pore confinements when χN decreases [60,61]. Here, the surface-induced ODT processes are observed to be the first-order because of the obvious changes on the free energy curves, accompanying the obvious structural alterations. In the surface-induced cases, the confinement entropy loss and interfacial energy have the contribution to the free energy for the diblock copolymers with the given χN according to Eq. (1), unlike the thermal-induced ODT cases where the enthalpic and entropic balance are determined by the incompatibility degree χN [1]. Although the surface-induced ODT processes are controlled by the strengths of surface field, the induced effects are analogous to the thermal-induced ODT process. Another characteristic is that the different preferential surfaces play distinct roles on inducing the ODT processes in two aspects. On the one hand, the A-preferential surface induces the monocontinuous phase, the SA_B-LN_A network structures, while the B-preferential surface induces the CN_A-CL_B phase with the bicontinuous network structure. On the other hand, the phase transition induced by B-preferential surfaces has a delay at the transition point from those by A-preferential surfaces. These ODTs are induced in the confinement environment by the preferential surface instead of the polymer parameters, which deepens our knowledge about the phase transitions in confined systems.

3.2. The OOTs in the arrays with large periods

It is expected to observe the novel phase structures and transitions of lamella-forming diblock copolymers in the nanoparticle arrays with large periods. The previous work have reported that the diblock copolymers exhibit complex phase structures and undergo a series of phase transition processes under the cylindrical and spherical confinements [24,30,46]. Here, we investigate the phase structures and the corresponding transition behaviors of diblock copolymers in the nanoparticle arrays with relatively large periods. The order phase structures observed are sorted into several groups, as shown in Fig. 4, and their transition behaviors are presented in Fig. 5. In order to observe the phase structures clearly, we plotted the three-dimensional structures by A and B segments distribution, and their cut views, respectively.

Fig. 4a show the SA_A-CL_A-CN_B phase structure. In this structure, the A-block domains are constructed by two-layer structures due to the relatively large confinement space. The outer layer in the calculation unit is eight spheres in the corner, constructing a cubically arranged sphere array (SA_A structure) in the whole nanoparticle array, while the inner layer is a concentric lamella (CL_A structure) near the nanoparticles with a weak connectivity with the neighboring nanoparticles at three directions. On the other hand, the B-block domain exhibits several cylinders connected each other at the edges of calculation unit, and constructs a cylinder network (CN_B structure) having a cubic symmetry in the whole array. Therefore, it is a bicontinuous structure packing a sphere array into a cubic arrangement in the whole nanoparticle array. Fig. 4b shows another phase structure, the SA_A-NL_A-HS_B structure. Similarly, the

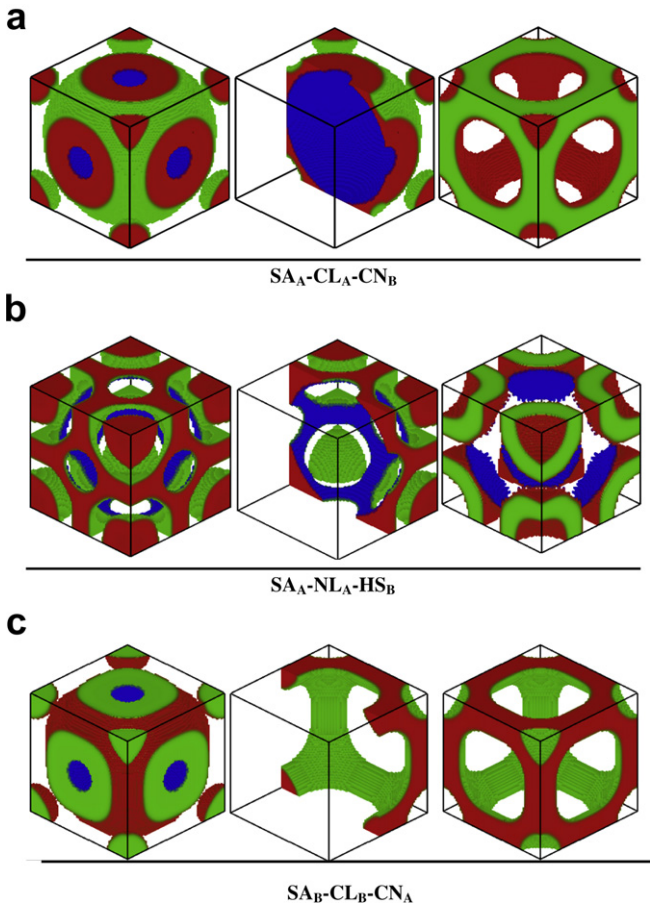

Fig. 4. The phase structures in the arrays with periods of $L = 3L_0$. (a) The SA_A-CL_A-CN_B monocontinuous structure. (b) The SA_B-NL_A-HS_B phase structure. (c) The SA_B-CL_B-CAN phases. The A-block and B-block domains are displayed, respectively.

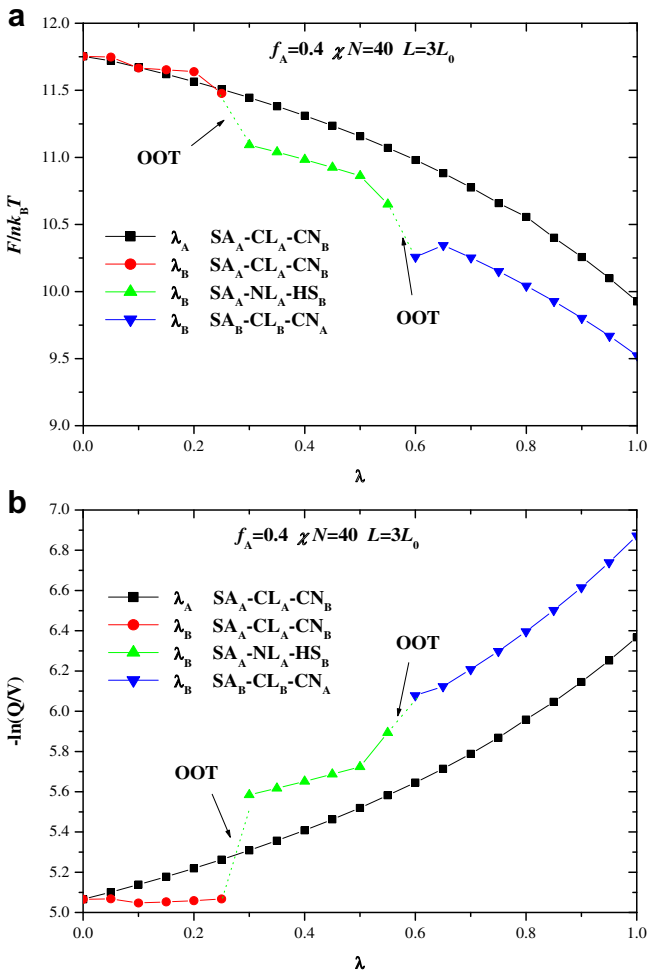

Fig. 5. The phase transitions induced by the surface fields in the arrays with periods of $L = 3L_0$ (a) The free energies, F/nk_BT, as functions of the strengths of surface preferences, λ_A and λ_B, respectively. (b) The entropic energies, $-\ln(Q/V)$, as functions of strengths of surface preferences, λ_A and λ_B, respectively.

A-block domain is a double layer where eight spheres appear in the corner of unit and composed of sphere array (SA_A structure) in the whole nanoparticle array. However, the inner layer is close to the nanoparticle surface and composed of the network lamellae (NL_A structure) in the whole array. The space between the inner and outer layers is filled with the B-block domain, exhibiting a hollow sphere (HS_B structure) array. Clearly, it is a monocontinuous structure where the B-blocks are separated with the inner and outer layers of A-blocks. In fact, the SA_A structure and HS_B structure combine into a two layers of solid sphere array. We have observed multilayer structures of diblock copolymers under the spherical confinements and nanorod-array confinements when the confinement size is increased [46,48]. It is reasonable to predict that the multilayer solid sphere might be observed in the nanoparticle arrays with the larger periods. It is interesting that we observe a SA_B-CL_B-CN_A phase structure, as shown in Fig. 4c. This SA_B-CL_B-CN_A structure is very similar to the SA_A-CL_A-CN_B structure shown in Fig. 4a. Although they have the similar domains, these domains are filled with the different blocks. It is worthy to point out that the preferential surfaces adsorb a layer of the corresponding block domain into the nanoparticle surfaces, resulting in a reversal of the SA_B-CL_B-CN_A structure to SA_A-CL_A-CN_B structure. The previous investigations reported the curving lamellae absorbing into the outer surfaces of nanoparticles [38]. Here, we observe two types of bicontinuous structures with the same patterns caused by the preferential surfaces. This observation reminds us that the different characteristic of nanomaterials may be fabricated with the same patterns.

These three phase structures obtained have several general characteristics. First, they all have the cubic symmetries, similar to the small period cases. This cubic symmetry is mainly due to the cubically arranged nanoparticles in the whole array, which requires the diblock copolymers inside having the cubic symmetry in the outer zones. Secondly, the nanoparticle surface has the spherical symmetry, and this fact requires the diblock copolymers inside have the spherical symmetry near the inner zones. These two different symmetries conflicts in their interfaces between the inner and outer zones, resulting in the complex phase structures. Another important characteristic is that the double-layer structures appear in the large period cases. All three types of phase structures exhibit the double layers for either A-blocks or B-blocks domains. The double layer attributes to the large periods while the single layer can be observed in the small period cases. In addition, the DIS phase cannot be observed in such large confinement space, which confirms our above argument that the small confinement space results in the DIS phase.

Then, we investigate the phase transitions of diblock copolymers in the nanoparticle arrays with large periods. We plotted the free energies and entropic energies as function of surface preference strength in Fig. 5. For the weak preferential surfaces, we observe the SA_A-CL_A-CN_B phase structures regardless of the surfaces either preferring to A-blocks or B-blocks. When $\lambda \leq 0.25$, the system

maintains the SA_A-CL_A-CN_B phase structure, which is independent of either A-preferential or B-preferential surfaces. This fact indicates that the phase structure is insensitive to the weak strength of surface preference. However, the different preferential surface behaves as distinct manners when the strength of surface preference is increased. As mentioned before, the A-block prefers to the neutral surface due to the hard-wall effect [59], which means that the structures in the arrays with A-preferential surfaces (the short-range interaction) is probably similar to those in the arrays with neutral surfaces. For the A-preferential surfaces, the free energy decreases smoothly as the preference strength is increased. This behavior indicates that there is not phase transition of diblock copolymers in the arrays with A-preferential surfaces, which is also confirmed by the fact that the diblock copolymers maintain the SA_A-CL_A-CN_B phase structure in the process. But, this is not the case in the B-preferential surfaces, as shown in Fig. 5a, which two jump points are observed in the free energy curve. These two jump points indicate that there are phase transitions when the strength of surface preference is increased. Obviously, these phase transitions are of first order, since the first-derivates of free energies are discontinuous. This first-order OOT accompanies an obvious structural transition in the process where the transition sequence is from SA_A-CL_A-CN_B to SA_A-NL_A-HS_B and then to SA_B-CL_B-CN_A. Here, the observations on the phase behaviors are similar to our recent study where the diblock copolymers undergo the first-order OOT for the diblock copolymers confined in the nanorod arrays [48]. But, we do not observe the second-order phase transition, unlike the cases of nanorod-array confinement. We also plotted entropic energies, $-\ln(Q/V)$, as function of surface preference strength, λ, in Fig. 5b. The curves further indicate that the phase transition is of first order. The increasing of entropic energies indicates that the system became more stable as λ increases, because the surface adsorbs the corresponding block more tightly for the increasing λ. This trend indicates that the effect of preferential surface not only induces the OOT processes, but also enhances the system stability in some sense. Here, the first-order OOTs of diblock copolymers in nanoparticle arrays have two characteristics which differ from those observed in the integral confinement-dimension cases. One is that the phases maintain the invariable symmetry, the cubic symmetry, in the surface-induced transition processes. However, the symmetry usually varies in the OOTs of diblock copolymers in the thin film, cylinder pore, and spherical cavity confinements. For example, the parallel lamellae structure can transit into the mix lamellae when the strength of surface preference increases [12]. The other is that the structural transition occurs between the monocontinuous and bicontinuous network structures during the OOT processes in the present work, however, there are not network structural transitions observed in the cylinder pores and spherical cavities due to the complete confinement in the certain directions [29,30,43,46].

It is necessary to summary the phase behaviors in the large period cases by comparing them to those in the small period cases. The similarity is in two aspects: one is that the order phases observed in their phase transitions are both the continuous network structures with cubic symmetries, either the bicontinuous structures or monocontinuous structures in the whole arrays; the other is about the phase transition order where the first-order phase transition are found in both cases by investigating the discontinuities in the first-derivative of free energy curves. Although these two cases have some similarities, the difference is obvious in several aspects. First, the ODT processes are only observed in the arrays with small periods, since the crowed space leads to the DIS phases while disappears in the relatively large space. However, the OOT processes are observed in the arrays with relatively large periods. Secondly, the slight asymmetry about the diblock plays different roles on the phase transitions in the large period arrays with the B-preferential and A-preferential surfaces. Namely, the OOTs can be induced by the B-preferential surfaces, which might be insensitive to the A-preferential surfaces in the large period cases. However, there are the ODTs are induced in the small period cases, in despite of either A-preferential or B-preferential surface.

4. Conclusion

We have preformed the SCFT calculations to study the surface-induced phase transitions of diblock copolymers in the nanoparticle arrays. The DIS phase and several continuous phases were observed in the arrays with the small and large periods, respectively, which differ from the other confinements. The complicated continuous phases include the SA_B-LN_A and SA_A-NL_A-HS_B monocontinuous phases and the CN_A-CL_B, SA_B-CL_B-CN_A and SA_A-CL_A-CN_B bicontinuous phases, exhibiting the cubic symmetries in the nanoparticle arrays, which can be understood based on the spherical symmetry originated from the nanoparticles and the cubic symmetry from the nanoparticle arrays. On the other hand, the surface-induced phase transitions between these observed phases were investigated by their free energies and entropic energies. In the arrays with small periods, the ODT sequence: DIS-(SA_B-LN_A) and (CN_A-CL_B) phases were observed for the A- and B-preferential surfaces, respectively. The surface-induced ODTs were different from those thermal-induced ODTs, which can be reasonably explained by the confinement effects. For the arrays with large periods, we observed the OOT sequence: (SA_A-CL_A-CN_B)-(SA_A-NL_A-HS_B)- (SA_B-CL_B-CN_A) for the B-preferential surfaces, in which the structures maintain the fixed cubic symmetry. Furthermore, the results indicate that the A- and B-preferential surfaces have the different induced effects because of the slight asymmetric diblock. The investigations on the free energies indicated that both the ODTs and OOTs are of first order in the surface-induced phase transition processes. The results on the entropic energy not only further confirm the first-order phase transitions in the ODTs and OOTs, but also indicate that the system becomes more stable when the strength of surface preference increases. Our observations reveal the novel phase structures in a distinct confinement system, which not only enrich our knowledge about the phase behaviors of macromolecules in confined systems, but also may be helpful to fabricate the novel nanomaterials.

Acknowledgments

This research was supported by the General Program of National Natural Science Foundation of China (Nos. 20774066, 20974081, 20934004, 50773072 and 20804001), the Outstanding Youth Fund of China (No.20525416), the National Basic Research Program of China (No.2005CB623800), and the Natural Science Foundation of Zhejiang Province, China (No.Y4090174).

References

[1] Ahn H, Ryu DY, Kim Y, Kwon KW, Lee J, Cho J. Macromolecules 2009;42:7897.
[2] Rodrígez-Hidalgo MR, Soto-Figueroa C, Matínez-Magadán JM, Vicente L. Polymer 2009;50:4596.
[3] Soto-Figueroa C, Rodrígez-Hidalgo MR, Matínez-Magadán JM, Vicente L. Macromolecules 2008;41:3297.
[4] Krausch G, Magerle R. Adv Mater 2002;14:1579.
[5] Park C, Yoon J, Thomas EL. Polymer 2003;44:6725.
[6] Wu Y, Cheng G, Katsov K, Sides SW, Wang J, Tang J, et al. Nat Mater 2004;3:816.
[7] Shin K, Xiang H, Moon SI, Kim T, McCarthy TJ, Russell TP. Science 2004;306:76.
[8] Kikuchi M, Binder K. J Chem Phys 1994;101:3367.
[9] Tang WH, Witten T. Macromolecules 1998;31:3130.
[10] Geisinger T, Muller M, Binder K. J Chem Phys 1999;111:5241.
[11] Wang Q, Yan Q, Nealey PF, de Pablo JJ. J Chem Phys 2000;112:450.
[12] Tang WH. Macromolecules 2000;33:1370.
[13] Guarini KW, Black CT, Yeung SHI. Adv Mater 2002;14:1290.
[14] Wang Q, Nealey PF, de Pablo JJ. Macromolecules 2003;36:1731.

[15] Xu T, Hawker CJ, Russell TP. Macromolecules 2005;38:2802.
[16] Angerman HJ, Johner A, Semenov AN. Macromolecules 2006;39:6210.
[17] Tsarkova L, Knoll A, Krausch G, Magerle R. Macromolecules 2006;39:3608.
[18] Chen D, Gong Y, Huang H, He T, Zhang F. Macromolecules 2007;40:6631.
[19] Eurich F, Karatchentsev A, Baschnagel J, Dieterich W, Maass P. J Chem Phys 2007;127:134905.
[20] Niihara K, Sugimori H, Matsuwaki U, Hirato F, Morita H, Doi M, et al. Macromolecules 2008;41:9318.
[21] Heckmann M, Drossel B. J Chem Phys 2008;129:214903.
[22] Heckmann M, Drossel B. Macromolecules 2008;41:7679.
[23] Di Z, Posselt D, Smilgies D-M, Papadakis CM. Macromolecules 2010;43:418.
[24] Chen P, Liang H, Shi A-C. Macromolecules 2007;40:7329.
[25] Xiang H, Shin K, Kim T, Moon SI, McCarthy TJ, Russell TP. Macromolecules 2004;37:5660.
[26] Xiang H, Shin K, Kim T, Moon SI, McCarthy TJ, Russell TP. Macromolecules 2005;38:1055.
[27] Feng J, Ruckenstein E. J Chem Phys 2006;125:164911.
[28] Feng J, Ruckenstein E. Macromolecules 2006;39:4899.
[29] Chen P, He X, Liang H. J Chem Phys 2006;124:104906.
[30] Yu B, Sun P, Chen T, Jin Q, Ding D, Li B. Phys Rev Lett 2006;96:138306.
[31] Li W, Wickham RA. Macromolecules 2006;39:8492.
[32] Wang Q. J Chem Phys 2007;126:024903.
[33] Yu B, Sun P, Chen T, Jin Q, Ding D, Li B, et al. J Chem Phys 2007;127:114906.
[34] Sevink GJA, Zvelindovsky AV. J Chem Phys 2008;128:084901.
[35] Yu B, Jin Q, Ding D, Li B, Shi A-C. Macromolecules 2008;41:4042.
[36] Li S, Wang X, Zhang L, Liang H, Chen P. Polymer 2009;50:5149.
[37] Yabu H, Higuchi T, Shimomura M. Adv Mater 2005;17:2062.
[38] Arsenault AC, Rider DA, Ttreault N, Chen JI-L, Coombs N, Ozin GA, et al. J Am Chem Soc 2005;127:9954.
[39] Cheng JY, Ross CA, Smith HI, Thomas EL. Adv Mater 2006;18:2505.
[40] Tanaka T, Saito N, Okubo M. Macromolecules 2009;42:7423.
[41] He X, Song M, Liang H, Pan C. J Chem Phys 2001;114:10510.
[42] Fraaije JGEM, Sevink GJA. Macromolecules 2003;36:7891.
[43] Yu B, Li B, Jin Q, Ding D, Shi A-C. Macromolecules 2007;40:9133.
[44] Feng J, Liu H, Hua Y. Fluid Phase Equilibria 2007;261:50.
[45] Higuchi T, Tajima A, Motoyoshi K, Yabu H, Shimonura M. Angew Chem Int Ed 2008;47:8044.
[46] Chen P, Liang H, Shi A-C. Macromolecules 2008;41:8938.
[47] Li S, Chen P, Wang X, Zhang L, Liang H. J Chem Phys 2009;130:014902.
[48] Wang X, Li S, Chen P, Zhang L, Liang H. Polymer 2009;50:4964.
[49] Wang Q, Nealey PF, de Pablo JJ. Macromolecules 2001;34:3458.
[50] Fredrickson GH, Ganesan V, Drolet F. Macromolecules 2002;35:16.
[51] Drolet F, Fredrickson GH. Phys Rev Lett 1999;83:4317.
[52] Matsen MW, Schick M. Phys Rev Lett 1994;72:2660.
[53] Matsen MW, Griffiths GH, Wickham RA, Vassiliev ON. J Chem Phys 2006;124:024904.
[54] Toombes GES, Finnefrock AC, Tate MW, Ulrich R, Wiesner U, Gruner SM. Macromolecules 2007;40:8974.
[55] Hajduk DA, Harper PE, Gruner SM, Honeker CC, Kim G, Thomas EL, et al. Macromolecules 1994;27:4063.
[56] Gao C, Sakamoto Y, Sakamoto K, Terasaki O, Che S. Angew Chem Int Ed 2006;45:4295.
[57] Benedicto AD, O'Brien DF. Macromolecules 1997;30:3395.
[58] Wohlgemuth M, Yufa N, Hoffman J, Thomas EL. Macromolecules 2001;34:6083.
[59] Meng D, Wang Q. J Chem Phys 2007;126:234902.
[60] Miao B, Yan D, Han CC, Shi A-C. J Chem Phys 2006;124:144902.
[61] Miao B, Yan D, Wickham RA, Shi A-C. Polymer 2007;48:4278.